New Phytologist

Research

Differences in biochemical, gas exchange and hydraulic response to water stress in desiccation tolerant and sensitive fronds of the fern *Anemia caffrorum*

Miquel Nadal[1], Tim J. Brodribb[2], Beatriz Fernández-Marín[3,4], José I. García-Plazaola[4], Miren I. Arzac[4], Marina López-Pozo[4], Alicia V. Perera-Castro[1], Javier Gulías[1], Jaume Flexas[1,5] and Jill M. Farrant[6]

[1]Research Group on Plant Biology under Mediterranean Conditions, Departament de Biologia, Universitat de les Illes Balears (UIB), INAGEA, Carretera de Valldemossa Km 7.5, Palma de Mallorca, Illes Balears 07122, Spain; [2]School of Natural Sciences, University of Tasmania, Hobart, Tas. 7001, Australia; [3]Department of Botany, Ecology and Plant Physiology, University of La Laguna (ULL), Tenerife 38200, Spain; [4]Department of Plant Biology and Ecology, University of the Basque Country (UPV/EHU), Barrio Sarriena s/n, Leioa 48940, Spain; [5]King Abdulaziz University, Jeddah 80200, Saudi Arabia; [6]Department of Molecular and Cell Biology, University of Cape Town, Private Bag X3, Rondebosch 7701, South Africa

Author for correspondence:
Miquel Nadal
Email: m.n.nadal92@gmail.com

Received: *22 November 2020*
Accepted: *23 April 2021*

New Phytologist (2021) **231:** 1415–1430
doi: 10.1111/nph.17445

Key words: *Anemia caffrorum*, desiccation tolerance, hydraulic conductance, lipophilic antioxidants, photosynthesis, pigments, water relations.

Summary

- Desiccation tolerant plants can survive extreme water loss in their vegetative tissues. The fern *Anemia caffrorum* produces desiccation tolerant (DT) fronds in the dry season and desiccation sensitive (DS) fronds in the wet season, providing a unique opportunity to explore the physiological mechanisms associated with desiccation tolerance.
- *Anemia caffrorum* plants with either DT or DS fronds were acclimated in growth chambers. Photosynthesis, frond structure and anatomy, water relations and minimum conductance to water vapour were measured under well-watered conditions. Photosynthesis, hydraulics, frond pigments, antioxidants and abscisic acid contents were monitored under water deficit.
- A comparison between DT and DS fronds under well-watered conditions showed that the former presented higher leaf mass per area, minimum conductance, tissue elasticity and lower CO_2 assimilation. Water deficit resulted in a similar induction of abscisic acid in both frond types, but DT fronds maintained higher stomatal conductance and upregulated more prominently lipophilic antioxidants.
- The seasonal alternation in production of DT and DS fronds in *A. caffrorum* represents a mechanism by which carbon gain can be maximized during the rainy season, and a greater investment in protective mechanisms occurs during the hot dry season, enabling the exploitation of episodic water availability.

Introduction

Vegetative desiccation tolerance is a distinct selective trait used by some land plants to cope with limited water availability (Proctor & Tuba, 2002). Desiccation tolerance is defined as the ability to recover full physiological functioning after surviving drying to leaf water potentials of *c.* −100 MPa (Alpert & Oliver, 2002), or after loss of 90–95% relative water content (*RWC*; Farrant *et al.*, 2007). Desiccation tolerance is relatively common among bryophytes but is rare in ferns and angiosperms (the so-called 'resurrection plants') and is absent in gymnosperms (Gaff & Oliver, 2013). While there is increasing evidence of individual differences among species in terms of the exact mechanisms of desiccation tolerance, there are many unifying features (Oliver *et al.*, 2020). Among these, the most ubiquitous mechanisms are the accumulation of sugars and late embryogenesis abundant proteins (LEAs), the maintained expression of antioxidant enzymes and increased antioxidant potential, and mechanical stabilization via vacuole fragmentation and cell wall folding (Hoekstra *et al.*, 2001; Farrant *et al.*, 2007; Fernández-Marín *et al.*, 2016; Oliver *et al.*, 2020). Protection of the photosynthetic apparatus during dehydration is also highly controlled, but the mechanisms used differ among species. Some monocots break down Chl and thylakoid membranes during drying in a set of features referred to as poikilochlorophylly (Tuba *et al.*, 1996; Sherwin & Farrant, 1998; Beckett *et al.*, 2012). However, all bryophytes, ferns and dicots are homoiochlorophyllous, in that they retain Chl and the internal structure of chloroplasts during dehydration to enable rapid resumption of photosynthesis on rehydration (reviewed in Farrant *et al.*, 2007; Oliver *et al.*, 2020). In such species, photodamage is prevented by Chl masking through leaf folding, reflective leaf hairs, anthocyanin accumulation (Muslin & Homann, 1992; Sherwin & Farrant, 1998; Farrant *et al.*, 2007), and production of lipophilic antioxidants such as zeaxanthin, tocopherols and carotenes (Kranner *et al.*, 2002; Fernández-Marín *et al.*, 2016; Oliver *et al.*, 2020).

Among desiccation tolerant plants, resurrection ferns constitute an interesting group due to their intermediate position between the more ancient and largely constitutive mechanisms present in bryophytes and the more derived features of resurrection angiosperms (Oliver *et al.*, 2000; López-Pozo *et al.*, 2018). There are currently 60–70 described species of desiccation tolerant ferns in the sporophyte phase (Oliver *et al.*, 2000) and an estimated further 200 to 1200 filmy ferns (Porembski, 2011). An extremely unusual example is the South African resurrection fern *Anemia caffrorum* (Gaff, 1977). *A. caffrorum* is a small fern (fronds *c.* 24–27 cm long) typically found along forest margins, often growing chasmophytically, in seasonally dry environments of the Northern, Western and Eastern Cape provinces of South Africa (Roux, 1995). This species shows foliar dimorphism or 'heteroblasty' (Zotz *et al.*, 2011), where the same individuals shift from producing desiccation tolerant (DT) fronds during the dry season to desiccation sensitive (DS) fronds during the rainy season (Farrant *et al.*, 2009). The nature of the fronds produced appears to be regulated by the rhizome, which remains DT throughout the year (Shoko, 2015). The mechanisms of desiccation tolerance in *A. caffrorum* have some similarities to those reported in resurrection angiosperms, in that they are induced during drying, rather than being constitutively expressed (Farrant *et al.*, 2009). These include frond curling, cell wall folding, and production of LEAs, heat stable proteins, sucrose, oligosaccharides and cyclitols (Farrant *et al.*, 2009). Desiccation sensitive fronds do not undergo these changes during dehydration, and extensive damage accrues during dehydration and subsequent rehydration (Farrant *et al.*, 2009). Thus *A. caffrorum* is an excellent model with which to explore the eco-physiological traits associated with desiccation tolerance by comparison between DS and DT fronds in the same species.

While the main physiological mechanisms conferring desiccation tolerance have been extensively characterized in several resurrection species (see Oliver *et al.*, 2020 for a comprehensive review), there have been few reports studying the 'cost' of the protective features used by resurrection plants in terms of the limited productivity associated with desiccation tolerant organisms (Alpert, 2006). In this regard, photosynthesis in combination with leaf structure, anatomy, and hydraulics, among other traits, have not yet been well characterised. Photosynthesis is one of the most sensitive processes to desiccation and, simultaneously, a source of oxidative damage as plants dehydrate (Dinakar *et al.*, 2012). A positive net CO_2 assimilation under relatively low water contents (40–50% *RWC*, depending on the species) has been reported, and the cessation of photosynthesis is possibly related to stomatal closure rather than inhibition of reactions of the photosynthetic apparatus (Schwab *et al.*, 1989; Peeva & Cornic, 2009; Rapparini *et al.*, 2015; Zia *et al.*, 2016). By contrast, the poikilochlorophyllous *Xerophyta* species shut down photosynthesis at higher *RWC* (55–60%) (Farrant, 2000; Mundree & Farrant, 2000; Beckett *et al.*, 2012). Nonetheless, to the best of our knowledge no study has reported in detail the photosynthetic limitations resulting from water deficit stress in resurrection plants (Nadal & Flexas, 2019) nor their possible coordination with leaf hydraulics (Flexas *et al.*, 2018). In this regard, *A. caffrorum* is a good candidate for testing the hypothesized trade-off between desiccation tolerance and productivity (Alpert, 2006). In line with our previous studies (Nadal *et al.*, 2018; Gago *et al.*, 2019), we propose that DT fronds would have a lower photosynthetic capacity because of the physiological, structural and anatomical features required for desiccation tolerance. To test this hypothesis, we assessed the water relations (and their possible structural/anatomical basis), hydraulics, photosynthetic capacity, and pigments and lipophilic antioxidants associated with photosynthesis, as well as abscisic acid content, in DT and DS fronds of *A. caffrorum*. The main objective of the present work is to compare these physiological features both under well-watered conditions and under water deficit stress. We applied photosynthesis and stomatal conductance models to discern the causes of their decline upon water loss and the possible differences between the two frond types. Finally, we discuss the possible consequences of adopting the mechanisms observed in DT fronds in relation to the ecophysiology of this species.

Material and Methods

Plant material and experimental design

Images of DT and DS plants and fronds of *Anemia caffrorum* (L.) Christenh. are shown in Fig. 1. Plants were collected during the end of the dry season in 2019 from Table Mountain in Cape Town (South Africa) when plants were naturally in their DT state with completely curled leaves (Fig. 1a,b). Individuals with recently developed leaves (determined by visual signs and rosette position) were placed in pots (width, 20 cm; depth, 10 cm) filled with soil from the site of collection and acclimated in growth chambers (Conviron, Percival, USA) under a 14 h : 10 h, light : dark photoperiod with a photosynthetic photon flux density (PPFD) of 800 μmol m^{-2} s^{-1}, at 28 : 24°C, and with optimum irrigation. Plants were acclimated to these conditions for 2 wk. For work on DS fronds, another set of plants was collected just before the start of the wet season. Desiccated plants were excavated from the field and acclimated in growth chambers under the same conditions described for DT plants. New fronds were produced after 1 month, and these had the typical DS phenotype (Fig. 1c), such as absence of orange/brown coloured abaxial hairs and lack of regulated frond curling upon dehydration (Fig. 1d–f; see Farrant *et al.*, 2009). After their respective acclimation times, measurements were performed on DT and DS plants for comparison under well-watered (WW) conditions. Although age could not be determined in DT fronds, fully developed fronds with no clear signs of ageing and/or stress were used in all cases. Subsequently, water deficit stress (WS) was imposed by withholding water for 2 wk. Plants were then kept for 1 wk in the dry state and rehydrated for 24 h. Stress monitoring and sample collection under both WW and WS conditions are detailed below (sub-sections 'Water status' and high performance liquid chromatography (HPLC) analyses).

Frond structure

Leaf mass per area (*LMA*) was determined in 16 replicates per frond type under WW conditions as described in Pérez-

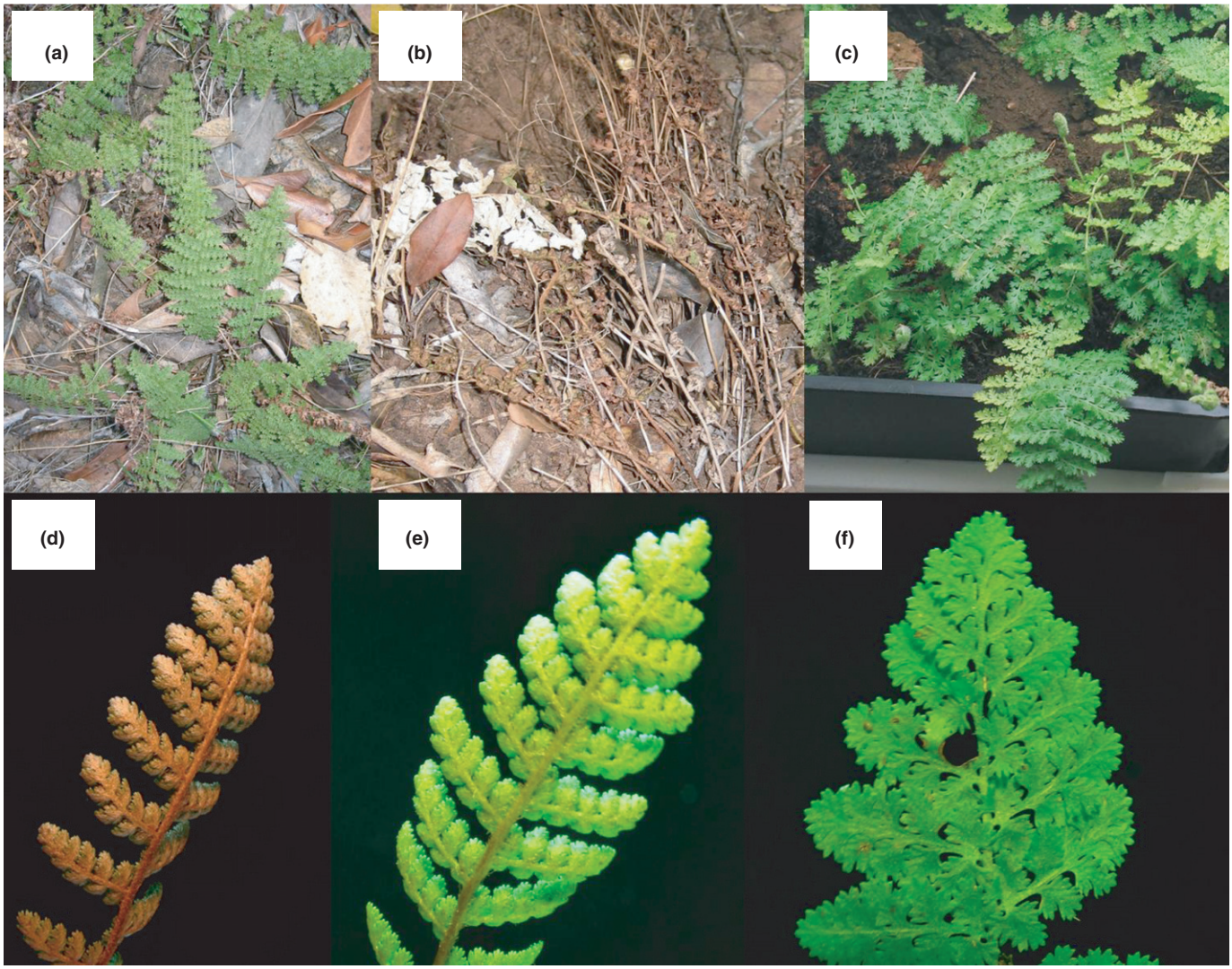

Fig. 1 Images of the resurrection fern *Anemia caffrorum*, including plants displaying desiccation tolerant (DT) and desiccation sensitive (DS) fronds. Desiccation tolerant plants in their natural environment on the slopes of Table Mountain, Cape Town, in hydrated (a) and dehydrated (b) states. Desiccation tolerant plants in growth chambers (c). Typical image of DT fronds (d), showing the brown colour given by abaxial hairs. Detail of the abaxial (e) and adaxial (f) surfaces of a DS frond.

Harguindeguy *et al.* (2013). The area of fully hydrated fronds (LA_{hy}) was measured using the ImageJ software (version 1.52p, Wayne Rasband, National Institutes of Health, USA, URL: http://imagej.nih.gov/ij/). Leaf dry mass (*DM*) was obtained after 72 h at 70°C. The area shrinkage or percentage loss of area in a dry frond (PLA_{dry}) was determined in seven replicates per frond type under WW conditions. Area shrinkage was calculated as $PLA_{dry} = (1–LA_{dry}/LA_{hy}) \times 100$ (Scoffoni *et al.*, 2014), where LA_{dry} is frond area measured after 72 h at 70°C.

Frond anatomy

Light and electron transmission microscopy were used for frond anatomy analysis under WW conditions. Five fronds per type were taken as replicates. Immediately after gas exchange measurements, small pieces (2 × 2 mm) were cut from the middle region of the same fronds (avoiding major veins). Frond material was fixed under vacuum with 4% glutaraldehyde and 2% paraformaldehyde in 0.1 M phosphate buffer and stored (4°C, dark) until subsequent preparation. Then, samples were post-fixed for 2 h in 2% buffered osmium tetroxide and dehydrated in a series of increasing ethanol concentrations. Dehydrated samples were embedded in Spurr's resin and solidified at 60°C for 48 h. Transverse semi-thin (0.8 μm) and ultra-thin (90 nm) sections were generated using an ultramicrotome. Semi-thin sections were stained with 1% toluidine blue, viewed at ×200 magnification using light microscopy (Olympus, Tokyo, Japan) and photographed with a Moticam 3 (Motic Electric Group Co., Xiamen, China). Ultra-thin sections were viewed at ×1500 and ×30 000 magnifications using transmission electron microscopy (TEM H600; Hitachi, Tokyo, Japan). All images were analysed using ImageJ.

The following parameters were obtained from light microscopy images (Tomàs *et al.*, 2013), as mean values of 10

measurements per individual (replicate): leaf thickness (*LT*), mesophyll thickness (*MT*), epidermis thickness (*ET*; sum of lower and upper epidermis thickness measurements), mesophyll fraction of intercellular air spaces (f_{ias}), and the thickness of the combination of epidermis cell wall and cuticle (T_{cwcut}), which was calculated as the mean between upper and lower epidermis measurements. From 10 ×1500 magnification images per replicate, the chloroplast surface area exposed to intercellular air spaces per area (S_c) was calculated as described in Evans *et al.* (1994) using the curvature correction factors from Thain (1983). Cell wall thickness of mesophyll cells (T_{cw}) was measured from 10 measurements per image in 10 images per replicate at ×30 000 magnification. Leaf density (*LD*) was calculated as *LMA/LT*.

Minimum conductance

Minimum leaf diffusion conductance to water vapor (g_{min}) was measured following Sack & Scoffoni (2011) under WW conditions. Eight fronds per type were collected at predawn and placed in the lab at a constant temperature (*c.* 24°C) for dehydration measures. Cut ends of fronds were sealed with a putty-like adhesive (Blu Tack; Bostik, Colombes, France). Fronds were gently swayed with a fan to minimize the boundary layer resistance. Frond mass was monitored over 2 h during which room temperature and humidity were recorded using an open gas exchange system (Li-6400XT; Li-Cor Inc., Lincoln, NE, USA) to calculate the vapour pressure deficit (*VPD*). g_{min} was obtained from the mass–time relationship as $g_{min} = E/VPD$, where E is the transpiration flux of water through the frond.

Photosynthesis measurements

An open gas exchange system with a coupled fluorescence chamber of 2 cm^2 (Li-6400XT; Li-Cor Inc.) was used to perform simultaneous measurements of gas exchange and Chl fluorescence. For all measurements, leakage in the sample–gasket interface was determined, and photosynthetic parameters were corrected accordingly (Flexas *et al.*, 2007). In eight replicates per frond type under WW conditions, light-saturated net assimilation (A_n), stomatal conductance to CO_2 (g_{sc}), substomatal CO_2 concentration (C_i) and photochemical yield of photosystem II (Φ_{PSII}) at chamber CO_2 (400 μmol mol^{-1}), saturating light (1000 μmol m^{-2} s^{-1}), ambient humidity (50–70%) and 25°C (block temperature), were recorded after reaching steady-state conditions (15–30 min). Subsequently, A_n–C_i curves were produced by increasing chamber CO_2 from 50 to 1500 μmol CO_2 mol^{-1} air in 14 steps every 3–4 min. From the A_n–C_i curves, the maximum velocity of Rubisco carboxylation (V_{cmax}), maximum electron rate (J_{max}), maximum rate of triose phosphate use (*TPU*) and mesophyll conductance to CO_2 (g_m) were determined using the curve-fitting method (Sharkey, 2016). The Rubisco kinetics of ferns reported in Gago *et al.* (2013) were used for model parameterization. Mitochondrial respiration in the dark (R_d) was measured in the same leaves after 20–30 min of dark adaptation.

Recordings of light-saturated A_n, stomatal conductance to water vapour (g_{sw}), and Φ_{PSII} after 10–15 min at ambient CO_2 (400 μmol mol^{-1}) were taken as instantaneous photosynthesis measurements each day during the WS treatment in both frond types between 10:00 and 16:00 h (lights on at 08:00 h). Under moderate WS (corresponding to a 50–60% decrease in g_{sw}), A_n–C_i curves were produced to determine the values of the photosynthesis parameters and limitations under such conditions. R_d and the maximum quantum yield of PSII (F_v/F_m) were also measured in the same leaves after dark-adaptation. Photosynthesis *relative* stomatal (l_s), mesophyll (l_m) and biochemical (l_b) limitations were estimated following the methods described by Grassi & Magnani (2005) under both WW and WS conditions. The slope at the Rubisco-limited portion of A_n–C_c (chloroplast CO_2 concentration) curves was used as a proxy for $\partial A/\partial C_c$. Stomatal (*SL*), mesophyll (*ML*) and biochemical (*BL*) contributions to A_n decrease were then calculated using values for WW conditions for each frond type as references.

Water status

Soil moisture, predawn and midday frond water potential (Ψ_{pd} and Ψ_{leaf}, respectively) and *RWC* were measured during WS, simultaneously with instantaneous gas exchange measurements. Soil moisture was assessed from three measurements per pot using a volumetric probe (WET-2 Sensor/HH2 Moisture Meter, Delta-T Devices, Cambridge, UK). Ψ_{pd} was measured on fronds from the same pot before dawn. After instantaneous gas exchange measurements, Ψ_{leaf} was measured after fronds reached equilibrium for 5–10 min in a sealed plastic bag. *RWC* was measured in the same frond, calculated as $(FM - DM) / (SM - DM) \times 100$, where *FM* is the fresh mass and *SM* is the water-saturated mass (obtained after overnight rehydration in distilled water). Water potential measurements were performed using a pressure chamber (Model 600D; PMS Instrument Co., Albany, NY, USA).

Photosynthetic response to rapid dehydration

The response of A_n, g_{sw} and Φ_{PSII} to rapid dehydration (1–2 h) was addressed following a similar procedure to that described by Trueba *et al.* (2019). Gas exchange and Chl fluorescence were measured in four DT and DS fronds under WW conditions as described in the 'Photosynthesis measurements' sub-section above. After reaching steady-state, values were recorded, and leaves were excised for (fresh) mass measurement. Afterwards, photosynthesis (for 3–5 min) and mass measurements were performed alternately until A_n approached 0 μmol m^{-2} s^{-1}. *RWC* was calculated using the estimated water-saturated mass from *SM/DM* obtained from pressure–volume (*P–V*) curves (see the following paragraph). The *RWC* at which A_n, g_{sw} and Φ_{PSII} decreased by 50% (RWC_{An-50}, RWC_{gsw-50} and $RWC_{\Phi PSII-50}$, respectively) were obtained by fitting polynomial regressions to their respective relationships with *RWC* (Supporting Information Fig. S1).

Pressure–volume curves

Pressure–volume measurements were performed following the bench-dry method (Sack & Pasquet-Kok, 2011). Six fronds per

type were measured under WW from initial predawn conditions. Each frond was dehydrated in the lab and alternately weighed and measured for water potential with the pressure chamber until a complete *P–V* curve with at least 10 points was obtained. The separation between full turgor and turgor loss (identifying the turgor loss point) was established, considering the highest r^2 of a linear fit for the linear portion of the $-1/\Psi$ vs $1-RWC$ relationship. From *P–V* curves, the following parameters were obtained: water potential (Ψ_{tlp}) and *RWC* (RWC_{tlp}) at turgor loss point, osmotic potential at full turgor (π_o), water-saturated mass per dry mass (*SM/DM*), leaf area-specific capacitance at full turgor ($C^*_{ft\text{-}area}$) and the bulk modulus of elasticity (ϵ). ϵ was calculated from total relative water content over the full range above RWC_{tlp} as described in Melkonian *et al.* (1982). The apoplastic water fraction (a_f) was calculated as the *x*-intercept of the $-1/\Psi$ vs *RWC* relationship.

Pressure–volume measurements were also performed in fronds under WS to explore possible osmotic adjustments once Ψ_{pd} decreased below −1 MPa. Fronds were measured from initial predawn conditions; nonetheless, in most cases it was possible to determine the turgor loss point. However, because few points were recorded above the turgor loss point, calculation of ϵ and $C^*_{ft\text{-}area}$ was not reliable in water-stressed fronds.

Hydraulic conductance

From instantaneous gas exchange and water status measurements, whole-plant leaf-specific hydraulic conductance (K_{plant}) was measured during WS using the evaporative flux method as described by Ramírez-Valiente *et al.* (2020), where $K_{plant} = E/(\Psi_{pd} - \Psi_{leaf})$. Transpiration flux ($E$) was taken from the Li-6400XT, and measured E was assumed to be representative of whole-frond E (Théroux-Rancourt *et al.*, 2015).

Application of the BMF model

The stomatal conductance model of Buckley *et al.* (2003) or 'BMF model' was applied to discern the contributions to g_{sw} decline under moderate WS, as described in a study by Rodriguez-Dominguez *et al.* (2016). Briefly, stomatal conductance to water vapor can be modelled with the following equation:

$$g_{sw} = \frac{na\,K_{plant}\,(\Psi_{soil} + \pi)}{K_{plant} + na\,\Delta w}$$

where π is bulk frond osmotic pressure, Δw is leaf-to-air water vapour mole fraction gradient and *na* comprises turgor-independent or 'nonhydraulic' effects, including possible hormone-driven stomatal control (n) and effects of light intensity and C_i on g_{sw} (a). Here, K_{plant}, Ψ_{soil} (approached by Ψ_{pd}), π and Δw were obtained experimentally from instantaneous gas exchange and water status measurements. π was determined by *P–V* curves from neighbouring fronds or from Ψ_{leaf} when $\Psi_{leaf} < \Psi_{tlp}$. The product *na* was fitted using 'Solver' in Microsoft Excel to minimize the sum of squares between measured and modelled g_{sw}. The percent contributions to g_{sw} decline of each model variable were calculated using the Excel tool provided by Rodriguez-Dominguez *et al.* (2016) following Buckley & Díaz-Espejo (2015). Values under WW conditions were used as a reference for each frond type.

High performance liquid chromatography analyses of photosynthetic pigments and tocopherols

Samples from the same fronds used for instantaneous gas exchange, Ψ_{leaf} and *RWC* measurements were excised immediately after measurement, snap frozen in liquid nitrogen, and stored at −80°C. Subsequently, samples were lyophilized under vacuum. Analyses were conducted on fronds of each type, taken from a complete range of *RWC* values during the WS cycle (n = 16–25). Approximately 15 mg of freeze-dried frond powder from each treatment was extracted in 0.5 ml of acetone 95% buffered with 0.5 g l^{-1} $CaCO_3$. Samples were centrifuged for 10 min at 16 100 ***g*** and the pellet was re-extracted in 0.5 ml of pure acetone. Extracts were centrifuged again, and the two supernatants were mixed and filtered through a 0.2 µm pore PTFE filter (Teknokroma, Spain). Photosynthetic pigments and tocopherols were then identified and quantified by HPLC (García-Plazaola & Becerril, 2001). Chlorophyll *a* and *b* content was expressed on an area basis using mean *LMA* for each frond type for its calculation.

Abscisic acid (ABA) analysis

Lyophilized samples collected before and during the WS cycle were used to determine ABA contents (n = 8). Leaf samples were covered in 80% (v/v) methanol in water and stored at −20°C for 24 h. After homogenization, ABA was stored at 4°C for another 24 h for extraction. At this stage, deuterated ABA was added as an internal standard. Subsequently, ABA purification and quantification was conducted using an ultra performance liquid chromatograph (UPLC) and multiple reaction-monitoring tandem mass spectrometry (MS) analysis (Waters Acquity H-series UPLC coupled to a Waters Xevo triple quadrupole mass spectrometer; BEH C18 column; Waters, Milford, CT, USA) as detailed in McAdam & Brodribb (2012). The amount of ABA was calculated as the amount of internal standard added multiplied by the ratio of endogenous ion intensity to internal standard ion intensity. The resulting ABA content was then adjusted for sample (dry) mass and aliquot volume.

Statistical analysis

All analyses were performed using the R statistical software (R Core Team, 2019) v.3.6.2. One-way ANOVA (function 'lm' of the stats package) was used for DT and DS comparison under WW conditions. Two-way ANOVA ('lm') was used for determining factor significance, including frond type and water conditions as factors. Linear or quadratic regressions were fit among continuous variables according to the Akaike information criterion (AIC); intercept and slope differences were determined by parametric ANCOVA ('lm') for linear fittings or by

nonparametric ANCOVA for quadratic fittings using the function 'T.aov' of the FANCOVA package (Wang, 2020).

Results

Frond comparison under well-watered conditions

Desiccation tolerant and desiccation sensitive fronds differed in their structure and in some anatomical parameters (Table 1). Notably, DT fronds showed a higher leaf mass per area and area shrinkage than DS fronds. The higher *LMA* was mainly driven by changes in leaf density (0.55 g cm^{-3} compared to 0.31 g cm^{-3} in DS) rather than differences in leaf thickness. Desiccation tolerant fronds also presented a lower ratio of epidermis to mesophyll thickness, a lower fraction of intercellular air spaces, and thinner epidermis cell walls (Table 1). No differences were detected in either chloroplast surface area or cell wall thickness. The higher tissue density of DT fronds is also reflected in their lower water-saturated mass per dry mass (Table 2). With respect to the pressure–volume parameters, DT fronds showed higher tissue elasticity (lower ϵ) and capacitance, whereas no differences were observed for osmotic potential at full turgor (Table 2). This resulted in similar osmotic potential but lower *RWC* at the turgor loss point in DT fronds.

Measurement of minimum conductance under well-watered conditions was hindered by the fact that transpiration progressively decreased as fronds dehydrated; hence, g_{min} is given as 'instantaneous' values in relation to *RWC* (Fig. 2). Desiccation tolerant and desiccation sensitive fronds differed in their g_{min}–*RWC* slopes ($P < 0.001$ for the interaction term). At the 80–90% *RWC* range, g_{min} values were 77.7 ± 8.4 for DT and 22.7 ± 2.4 mmol m^{-2} s^{-1} for DS. The dependence of g_{min} on *RWC* may imply that stomata were not completely closed for a substantial *RWC*; hence, we did not correct stomatal conductance for cuticular conductance as done in similar studies (e.g. Théroux-Rancourt *et al.*, 2015). Nonetheless, we did not detect significant discrepancies when considering g_{min} in the gas exchange-derived parameters (data not shown). Desiccation tolerant fronds showed lower net assimilation than DS fronds (7.59 ± 0.88 compared to 9.70 ± 0.61 μmol m^{-2} s^{-1}); this arises mainly as a result of lower biochemical capacity (V_{cmax}, J_{max}) and mesophyll conductance (Table 3). On the other hand, stomatal conductance was higher in DT fronds, which results in their lower WUE_i. Indeed, *relative* limitation analysis showed that photosynthesis in DT fronds was less limited by g_{sc} (lower l_s; Table 4) under WW conditions, and showed a slightly higher l_m. However, biochemical limitations accounted for half of photosynthesis limitations in both frond types (l_b = 0.51–0.52).

No differences were detected in total Chl content nor in the Chl*a* : Chl*b* ratios between frond types (Table 5). On the other hand, DT fronds had significantly higher β-carotene : Chl and β-carotene : neoxanthin ratios than DS fronds. Despite nonsignificant differences among frond types in total amount of xanthophyll cycle pigments (*VAZ* : Chl), DT fronds showed enhanced ratios of lipophilic antioxidants to Chl. This was characterised by higher β-carotene and more than threefold higher α-carotene, α-tocopherol and γ-tocopherol content per Chl (Table 5).

Response to water deficit stress

Soil moisture decreased at a similar rate for all plants (Fig. S2). Predawn water potential decreased to −1 MPa by day 8–9, after which *RWC*, Ψ_{leaf}, hydraulic conductance and A/C_i monitoring was initiated until day 13–14, when Ψ_{leaf} was below −4 MPa and curling in DT fronds made gas exchange measurements difficult. Desiccation tolerant and desiccation sensitive fronds showed a similar photosynthesis response under moderate water stress conditions (days 7–13 of the water deficit stress cycle), where all parameters but water use efficiency decreased in both frond types (Table 3). WUE_i, increased in DS fronds under progressive dehydration but did not change in DT fronds. In DT fronds, biochemical limitations (27 ± 3%) were the main cause of A_n reduction compared to WW conditions, whereas both stomatal (22 ± 2%) and biochemical limitations (19 ± 3%) contributed significantly to the A_n decrease observed in DS fronds (Table 4). Diffusive limitations (*SL* + *ML*) accounted for 18 and 33% of the reductions in A_n observed in DT and DS fronds, respectively, with *ML* being higher than *SL* in DT fronds (Table 4). No changes in Chl*a* or Chl*b* content were detected under WS.

After 1 wk, when the average *RWC* of fronds remained at < 25%, plants were rewatered. After 24 h, DT fronds showed high F_v/F_m (0.677 ± 0.022) and a slight recovery in A_n (2.75 ± 0.69 μmol m^{-2} s^{-1}) and g_{sc} (0.142 ± 0.039 mol m^{-2} s^{-1}). There was no recovery of photosynthetic activity in DS fronds. Notably, recovery in DT fronds required both high soil water and air humidity. Dehydration–rehydration tests on excised fronds showed that *RWC* recovery was not possible when fronds were rehydrated with distilled water through the petiole under

Table 1 Structure and anatomy of desiccation sensitive (DS) and desiccation tolerant (DT) fronds of *Anemia caffrorum* under well-watered conditions.

Frond		*LMA* (g m^{-2})	PLA_{dry} (%)	*LT* (μm)	*E/M T*	f_{ias} (%)	T_{cwcut} (μm)	S_c (m m^{-2})	T_{cw} (nm)
DS		46.1 ± 1.6	48.8 ± 4.5	149.4 ± 13.0	0.42 ± 0.01	37.5 ± 3.9	3.40 ± 0.09	4.59 ± 0.69	685 ± 90
DT		95.5 ± 3.0	63.8 ± 1.5	173.8 ± 25.1	0.32 ± 0.03	25.2 ± 3.3	2.71 ± 0.10	8.11 ± 2.07	592 ± 49
ANOVA	*F*	190.6	9.83	0.75	6.66	5.89	25.2	2.61	0.85
	P	< 0.001	0.009	0.412	0.033	0.042	0.001	0.145	0.385

E/M T, epidermis to mesophyll thickness ratio; f_{ias}, fraction of intercellular air spaces; *LMA*, leaf mass per area; *LT*, leaf thickness; PLA_{dry}, area shrinkage or percentage loss of area in a dry frond; S_c, chloroplast surface area exposed to intercellular air spaces per area; T_{cw}, mesophyll cell wall thickness; T_{cwcut}, combined thickness of the epidermis cell wall and cuticle. One-way ANOVA for frond type effect; mean ± SE.

Table 2 Water relations parameters derived from pressure–volume curves of desiccation sensitive (DS) and desiccation tolerant (DT) fronds of *Anemia caffrorum* under well-watered conditions.

Frond		*SM/DM* ($g\ g^{-1}$)	π_o (MPa)	π_{tlp} (MPa)	RWC_{tlp} (%)	ϵ (MPa)	$C^*_{ft\text{-}area}$ ($mol\ m^{-2}\ MPa^{-1}$)	a_f
DS		3.98 ± 0.20	−1.43 ± 0.06	−1.52 ± 0.07	95.7 ± 0.2	31.9 ± 1.6	0.24 ± 0.01	0.20 ± 0.02
DT		2.47 ± 0.04	−1.31 ± 0.17	−1.77 ± 0.18	80.1 ± 2.7	8.2 ± 2.2	1.09 ± 0.28	0.21 ± 0.06
ANOVA	*F*	63.6	0.38	1.48	27.9	69.8	7.77	0.01
	P	< 0.001	0.549	0.249	< 0.001	< 0.001	0.018	0.917

ϵ, bulk modulus of elasticity; π_o, osmotic potential at full turgor; π_{tlp}, osmotic potential at turgor loss point; a_f, apoplastic water fraction; $C^*_{ft\text{-}area}$, leaf area specific capacitance at full turgor; RWC_{tlp}, relative water content at turgor loss point; *SM/DM*, water-saturated mass per dry mass. One-way ANOVA for frond type effect; mean ± SE.

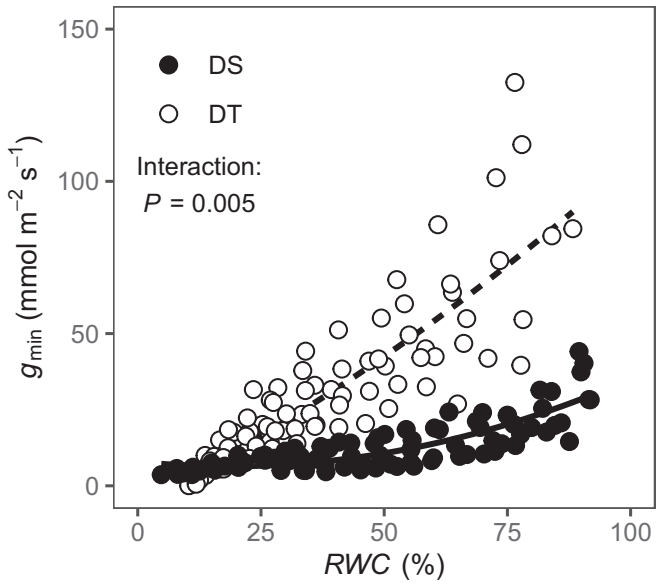

Fig. 2 Minimum conductance to water vapour (g_{min}) plotted against relative water content (*RWC*) measured in fronds of *Anemia caffrorum* under well-watered conditions. Filled circles correspond to desiccation sensitive (DS) fronds and open circles to desiccation tolerant (DT) fronds. Differences among frond types assessed using non-parametric ANCOVA: significant slope difference ($P = 0.005$) in quadratic fittings for DS (solid line, $r^2 = 0.67$, $P < 0.001$) and DT (dashed line, $r^2 = 0.76$, $P < 0.001$).

ambient humidity (*c.* 50%); they also required water vapour saturation for full rehydration (Fig. S3).

The relationships between photosynthesis parameters, hydraulics and water status are shown in Fig. 3. A_n, F_v/F_m and K_{plant} decreased in a similar manner in response to lowering of *RWC* and Ψ_{leaf} in both DS and DT fronds. By contrast, the response of stomatal conductance differed between DT and DS fronds. The relationship between g_{sw} and *RWC* (Fig. 3b) depended on frond type (ANCOVA, $P < 0.010$ for the interaction term). Similarly, the relationship between g_{sw} and Ψ_{leaf} (Fig. 3e) differed between DT and DS fronds (ANCOVA, $P = 0.005$ for frond type). These differences in the stomatal response are also reflected in the relationship with A_n (Fig. 3g), where the relationship between A_n and g_{sw} depended on frond type (ANCOVA, $P = 0.005$ for the interaction term), and the relationship with hydraulic conductance (Fig. 3h), where DT fronds showed higher g_{sw} per K_{plant} (ANCOVA, $P < 0.001$ for the intercept). Both fronds showed the same A_n–K_{plant} relationship (Fig. 3i). The different response of g_{sw} to *RWC* depending on frond type can also be observed in fronds from WW plants excised and subjected to rapid dehydration, where RWC_{gsw-50} was 35.2 ± 4.6% in DT fronds and 81.9 ± 5.5% in DS fronds (Table S1). The contributions to moderate g_{sw} decline (decrease of 35–45%) differed between DT and DS fronds (Table 6). The decline of K_{plant} had a greater effect on g_{sw} in DT (−115%) than in DS fronds (−48%). This negative effect of K_{plant} in DT fronds was partially compensated for by larger increases in osmotic pressure (changes in π of 135% as compared to 53% in DS fronds). A significant portion of the decline in g_{sw} was attributed to lower soil water potential in both frond types (*c.* −100%). The overall contribution of turgor-independent factors was minimal (−8–6% for *na*). Only a slight decrease of osmotic potential at full turgor was detected under WS conditions for both DS and DT fronds, from −1.37 MPa (mean of both frond types) to −1.71 MPa (two-way ANOVA, $P = 0.052$ for factor 'water').

Abscisic acid content per dry mass increased > 20-fold in response to moderate water stress (40–60% *RWC*) in both DT and DS fronds (Fig. 4a). This increase in ABA was negatively related to g_{sw} at this water stress range (Fig. 4b); however, ABA concentrations in the dry leaves (*RWC* < 25%) were only slightly higher than those at the WW stage. The de-epoxidation state of the xanthophyll cycle pigments (*AZ* : *VAZ*) and tocopherols were strongly affected by water deficit stress, and their responses differed among frond types (Fig. 5). While a similar rise in *AZ* : *VAZ* was observed in both DT and DS fronds as *RWC* decreased (Fig. 5a), DT fronds showed a slightly higher zeaxanthin content per Chl (Fig. 5b) at lower *RWC* compared to DS fronds (ANCOVA, $P = 0.009$ for the interaction term). Similarly, DT fronds had higher α-tocopherol (Fig. 5c) and γ-tocopherol per Chl (Fig. 5d) under both WW and WS conditions. Both α- and γ-tocopherols showed a significant increase during dehydration that was much more prominent in DT fronds (ANCOVA, $P = 0.001$ for the interaction term), especially in the case of γ-tocopherol.

Discussion

Distinctive frond structure and photosynthesis

In the present study we were able to ascertain common and distinctive physiological features of DT and DS fronds of

Table 3 Photosynthetic parameters of desiccation sensitive (DS) and desiccation tolerant (DT) fronds of *Anemia caffrorum* under well-watered (WW) and water deficit stress (WS) conditions.

Frond			A_n (μmol m^{-2} s^{-1})	g_{sc} (mol m^{-2} s^{-1})	WUE_i (μmol mol^{-1})	Φ_{PSII}	V_{cmax} (μmol m^{-2} s^{-1})	J_{max} (μmol m^{-2} s^{-1})	TPU (μmol m^{-2} s^{-1})	g_m (mol m^{-2} s^{-1})
DS	WW		9.70 ± 0.61	0.189 ± 0.013	31.6 ± 1.8	0.211 ± 0.010	40.4 ± 4.5	67.7 ± 4.2	4.75 ± 0.30	0.110 ± 0.010
DT	WW		7.59 ± 0.88	0.233 ± 0.016	19.8 ± 2.0	0.193 ± 0.026	30.3 ± 4.7	57.4 ± 5.5	4.06 ± 0.35	0.077 ± 0.011
DS	WS		5.18 ± 0.55	0.053 ± 0.006	64.4 ± 4.7	0.128 ± 0.012	23.9 ± 2.2	46.2 ± 3.9	2.98 ± 0.25	0.070 ± 0.010
DT	WS		4.15 ± 0.38	0.128 ± 0.011	20.4 ± 1.5	0.113 ± 0.008	16.1 ± 1.6	37.0 ± 2.3	2.56 ± 0.26	0.050 ± 0.006
ANOVA	D	*F*	6.15	26.6	137.1	1.60	9.71	7.00	3.56	7.42
		P	0.017	< 0.001	< 0.001	0.213	0.003	0.011	0.068	0.009
	W	*F*	50.4	70.1	11.02	39.5	32.9	34.7	33.8	14.8
		P	< 0.001	< 0.001	0.002	< 0.001	< 0.001	< 0.001	< 0.001	< 0.001
	W×D	*F*	0.82	1.38	29.0	0.01	0.02	0.02	0.22	0.48
		P	0.371	0.245	< 0.001	0.917	0.695	0.887	0.642	0.492

Φ_{PSII}, photochemical yield of photosystem II; A_n, light-saturated net CO_2 assimilation; g_m, mesophyll conductance to CO_2; g_{sc}, stomatal conductance to CO_2; J_{max}, maximum electron transport rate; *TPU*, maximum rate of triose phosphate use; V_{cmax} maximum velocity of Rubisco carboxylation; WUE_i, intrinsic water use efficiency. Two-way ANOVA including frond type (D) and water status (W) effects; mean ± SE.

Table 4 Photosynthesis limitations of desiccation sensitive (DS) and desiccation tolerant (DT) fronds of *Anemia caffrorum* under well-watered (WW) and water stress (WS) conditions, estimated from the parameters depicted in Table 3.

Frond			l_s	l_m	l_b	*SL* (%)	*ML* (%)	*BL* (%)
DS	WW		0.17 ± 0.01	0.31 ± 0.04	0.52 ± 0.05	0	0	0
DT	WW		0.11 ± 0.01	0.38 ± 0.06	0.51 ± 0.06	0	0	0
DS	WS		0.30 ± 0.02	0.25 ± 0.02	0.45 ± 0.03	22.3 ± 2.4	10.9 ± 3.1	18.5 ± 2.9
DT	WS		0.11 ± 0.01	0.31 ± 0.03	0.59 ± 0.03	4.7 ± 1.2	13.2 ± 3.8	27.7 ± 3.6
ANOVA	D	*F*	116.5	2.89	4.67	17.4	2.63	7.83
		P	< 0.001	0.096	0.036	< 0.001	0.111	0.007
	W	*F*	6.61	2.18	0.26			
		P	0.014	0.147	0.610			
	W×D	*F*	22.5	0.01	3.09			
		P	< 0.001	0.925	0.086			

Relative stomatal (l_s), mesophyll (l_m) and biochemical (l_b) limitations; and contributions of stomata (*SL*), mesophyll (*ML*) and biochemistry (*BL*) to A_n decline, taking WW values as reference for each frond type. Two-way ANOVA including frond type (D) and water status (W) effects for l_s, l_m and l_b; one-way ANOVA for frond type effect for *SL*, *ML* and *BL* under WS conditions; mean ± SE.

Table 5 Pigment and lipophilic antioxidants content of desiccation sensitive (DS) and desiccation tolerant (DT) fronds of *Anemia caffrorum* under well-watered conditions.

Frond		Chl *a* + *b* (μmol m^{-2})	Chl *a* : Chl *b* (mol mol^{-1})	*VAZ* : Chl (mmol mol^{-1})	α-carot : Chl (mmol mol^{-1})	β-carot : Chl (mmol mol^{-1})	β-carot : Neo (mmol mol^{-1})	Total toc : Chl (mmol mol^{-1})
DS		187.1 ± 24.3	2.40 ± 0.11	35.0 ± 3.4	1.23 ± 0.16	61.8 ± 3.9	1.32 ± 0.06	23.4 ± 7.1
DT		251.3 ± 26.7	2.55 ± 0.09	41.2 ± 6.3	4.42 ± 0.80	76.7 ± 3.2	1.66 ± 0.14	140.0 ± 32.8
ANOVA	*F*	3.15	1.15	0.84	18.5	8.46	5.54	14.5
	P	0.110	0.313	0.383	0.002	0.017	0.043	0.004

α-carot : Chl, α-carotene per Chl; β-carot : Chl, β-carotene per Chl; β-carot : Neo, β-carotene per neoxanthin; Chl *a* + *b*, chlorophyll *a* and *b* content per area; Chl *a* : Chl*b* chlorophyll a and b ratio; Total toc : Chl, total tocopherols (α- and γ-tocopherols) per Chl; *VAZ*/Chl, total amount of xanthophyll cycle pigments per Chl. One-way ANOVA for frond type effect; mean ± SE.

A. caffrorum under WW and WS conditions. In a previous study on this species, which did not include photosynthetic measurements, Farrant *et al.* (2009) did point to some structural differences between DT and DS that may affect the ecophysiology of this plant. The higher specific leaf area (i.e. the inverse of *LMA*) in DS fronds was regarded as indicative of a higher photosynthetic efficiency over the DT fronds. Indeed, in the present study we also observed the same differences in *LMA* and a larger A_n in DS than in DT fronds under well-watered conditions. Photosynthesis in DT fronds was lower due to a combination of

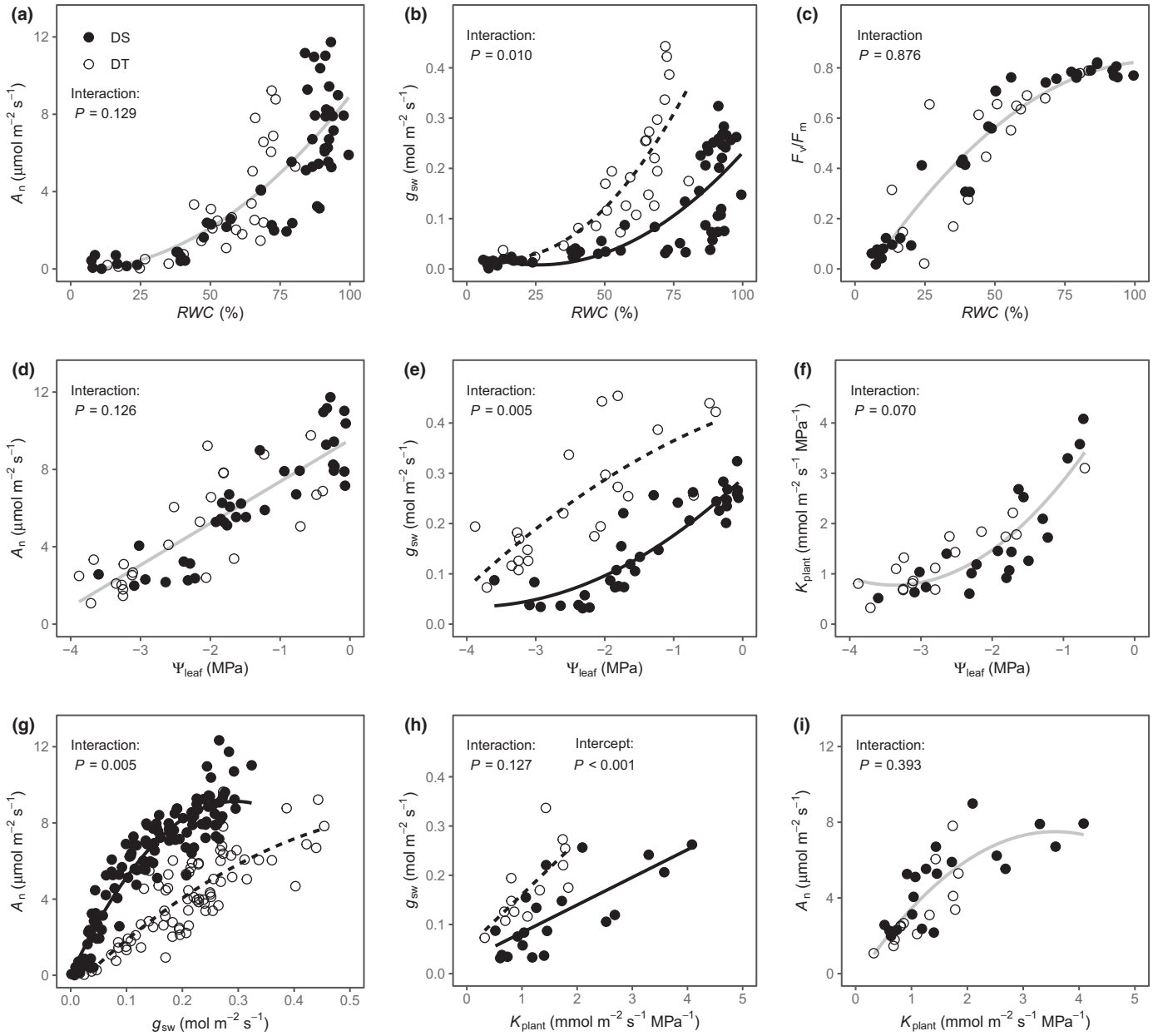

Fig. 3 Relationships between photosynthesis parameters, hydraulics, and water status of desiccation sensitive (DS) and desiccation tolerant (DT) fronds of *Anemia caffrorum* under water deficit stress. Filled circles correspond to DS fronds and open circles to DT fronds. The significance of the interaction (slope) and frond type (intercept) effects was determined using parametric ANCOVA and non-parametric ANCOVA for linear and quadratic fittings, respectively. Net CO_2 assimilation (A_n) and relative water content (*RWC*; a): no differences among frond types; quadratic fitting for pooled data ($r^2 = 0.70$, $P < 0.001$). Stomatal conductance to water vapour (g_{sw}) and *RWC* (b): significant differences among frond types; quadratic fittings for DS (solid line, $r^2 = 0.60$, $P < 0.001$) and DT (dashed line, $r^2 = 0.60$, $P < 0.001$). Maximum quantum yield of PSII (F_v/F_m) and *RWC* (c): no differences among frond types; quadratic fitting for pooled data ($r^2 = 0.87$, $P < 0.001$). A_n and frond water potential (Ψ_{leaf}; d): no differences among frond types; linear fitting for pooled data ($r^2 = 0.72$, $P < 0.001$). g_{sw} and Ψ_{leaf} (e): significant differences among frond types; quadratic fittings for DS (solid line; $r^2 = 0.79$, $P < 0.001$) and DT (dashed line; $r^2 = 0.61$, $P < 0.001$). Whole-plant leaf-specific hydraulic conductance (K_{plant}) and Ψ_{leaf} (f): no differences among frond types; quadratic fitting for pooled data DS ($r^2 = 0.76$, $P < 0.001$). A_n and g_{sw} (g): significant differences among frond types; quadratic fittings for DS (solid line; $r^2 = 0.88$, $P < 0.001$) and DT (dashed line; $r^2 = 0.70$, $P < 0.001$). g_{sw} and K_{plant} (h): significant differences among frond types; linear fittings for DS (solid line; $r^2 = 0.52$, $P < 0.001$) and DT (dashed line; $r^2 = 0.49$, $P = 0.005$). A_n and K_{plant} (i): no differences among frond types; quadratic fitting for pooled data ($r^2 = 0.63$, $P < 0.001$).

biochemical (V_{cmax}, J_{max}) and diffusive (g_m) limitations, compared to DS fronds. Mesophyll conductance is strongly limited by mesophyll cell wall thickness and chloroplast distribution (Terashima *et al.*, 2011; Onoda *et al.*, 2017). However, in this species, DT and DS fronds showed comparable S_c and T_{cw}. The reduced biochemical capacity in DT fronds could be explained by a lower nitrogen investment in the photosynthetic apparatus, including lower Rubisco content – one of the most important N

Table 6 Contributions to stomatal conductance decline under water deficit stress in desiccation sensitive (DS) and desiccation tolerant (DT) fronds of *Anemia caffrorum*.

Frond		Ψ_{pd} (MPa)	$p\ g_{sw}$ (%)	$p\ na$ (%)	$p\ \Psi_{soil}$ (%)	$p\ \pi$ (%)	$p\ K_{plant}$ (%)	$p\ \Delta w$ (%)
DS		−1.14 ± 0.14	−35.9 ± 3.1	5.9 ± 3.0	−95.0 ± 12.9	53.2 ± 19.1	−47.8 ± 20.0	−16.3 ± 4.3
DT		−1.37 ± 0.19	−45.5 ± 5.7	−7.9 ± 5.3	−106.0 ± 22.1	134.5 ± 24.3	−115.3 ± 21.2	−5.2 ± 4.0
ANOVA	*F*	1.05	2.34	5.60	0.20	7.12	5.37	3.56
	P	0.329	0.155	0.037	0.664	0.022	0.041	0.086

Percent parameters refer to either DS or DT fronds under well-watered conditions. Ψ_{pd}, pre-dawn water potential of the plants included in the modelling; $p\ \Delta w$, leaf-to-air water vapour mole fraction difference; $p\ \pi$, frond osmotic pressure; $p\ \Psi_{soil}$, soil water potential; $p\ g_{sw}$, total percent decline in stomatal conductance to water vapour; $p\ K_{plant}$, whole-plant leaf-specific hydraulic conductance; $p\ na$, percent contributions of leaf turgor-independent parameters. The total decline of g_{sw} is explained by the sum of the contributions; negative signs indicate an effect towards diminishing g_{sw}, whereas positive signs indicate the opposite effect. One-way ANOVA for frond type effect; mean ± SE.

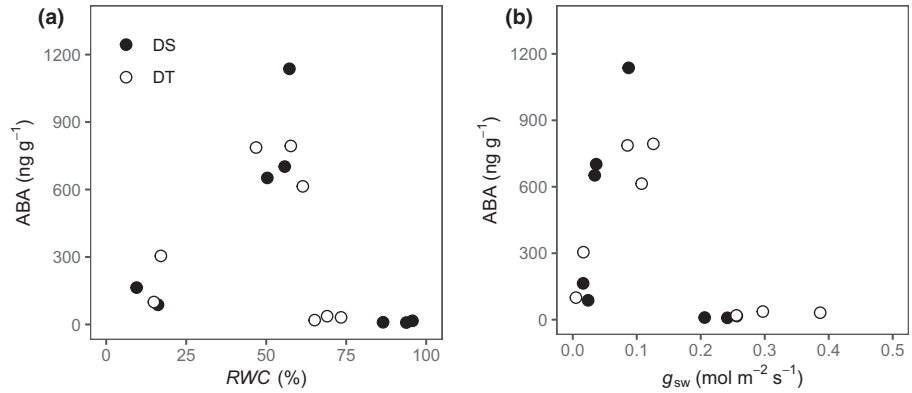

Fig. 4 Changes in abscisic acid (ABA) content per dry mass in relation to frond relative water content (*RWC*; a) and stomatal conductance to water vapour (g_{sw}; b) under water deficit stress. Closed circles correspond to desiccation sensitive (DS) fronds and open circles to desiccation tolerant (DT) fronds of *Anemia caffrorum*.

pools in leaves (Evans & Clarke, 2019) – and/or activation, which is reflected in the lower V_{cmax} of DT fronds. Nonetheless, both fronds showed similar Chl content, and hence the structural and biochemical basis of the different photosynthetic capacity are not clear. The higher *LMA* and leaf density of DT fronds was, however, not reflected in their pressure–volume parameters, as indeed they showed higher tissue elasticity and capacitance, despite the association between leaf density and ϵ (Niinemets, 2001; Saito *et al.*, 2006). Furthermore, DT leaves have a higher degree of shrinkage, a common feature of resurrection plants (Vicré *et al.*, 2004; Moore *et al.*, 2013; López-Pozo *et al.*, 2018; Shivariaj *et al.*, 2018), which is associated with tissue elasticity (Scoffoni *et al.*, 2014). Indeed, comparison of wall composition of DT and DS fronds of this species has shown that there is considerably more arabinose (15–20%) in DT than DS fronds (Moore *et al.*, 2013). Arabinose polymers and in particular arabinogalactan proteins seem to be related to wall flexibility in resurrection plants (Moore *et al.*, 2013; Shivaraj *et al.*, 2018; Oliver *et al.*, 2020). The higher elasticity of DT fronds could also be a product of their higher proportion of more flexible mesophyll tissues and thinner epidermis cell walls, as reported by Onoda *et al.* (2015). High elasticity in resurrection species prevents cytorrhesis and subcellular damage during desiccation (Moore *et al.*, 2008). The distinct photosynthetic and structural features among frond types point towards a greater efficiency in productivity of DS fronds (higher photosynthetic capacity and lower leaf investment) compared to DT fronds.

Different stomatal conductance responses under stress

Both g_{sw} and g_{min} were higher in DT fronds under WW conditions; these differences in g_{sw} were maintained under WS, showing that DT fronds present either an incomplete stomatal closure and/or high cuticle conductance and thus greater water loss compared to DS fronds. However, higher g_{sw} per *RWC* and Ψ_{leaf} of DT fronds did not appear to contribute to greater CO_2 assimilation, as deduced from the higher water use efficiency of DS fronds. Photosynthesis in DT fronds was mainly limited by biochemical factors, contrary to most plants where stomatal and mesophyll limitations are generally higher (Nadal & Flexas, 2019). The decrease in stomatal conductance is driven by turgor-related effects (Rodriguez-Dominguez *et al.*, 2016), among which hydraulic conductance is thought to play a predominant role (Wang *et al.*, 2018). Indeed, K_{plant} reduction was the main factor determining g_{sw} decline, although the hydraulic effect on decreasing turgor was ameliorated by lower osmotic potential during dehydration, especially in DT fronds. The compensation through osmotic pressure could be attributed to

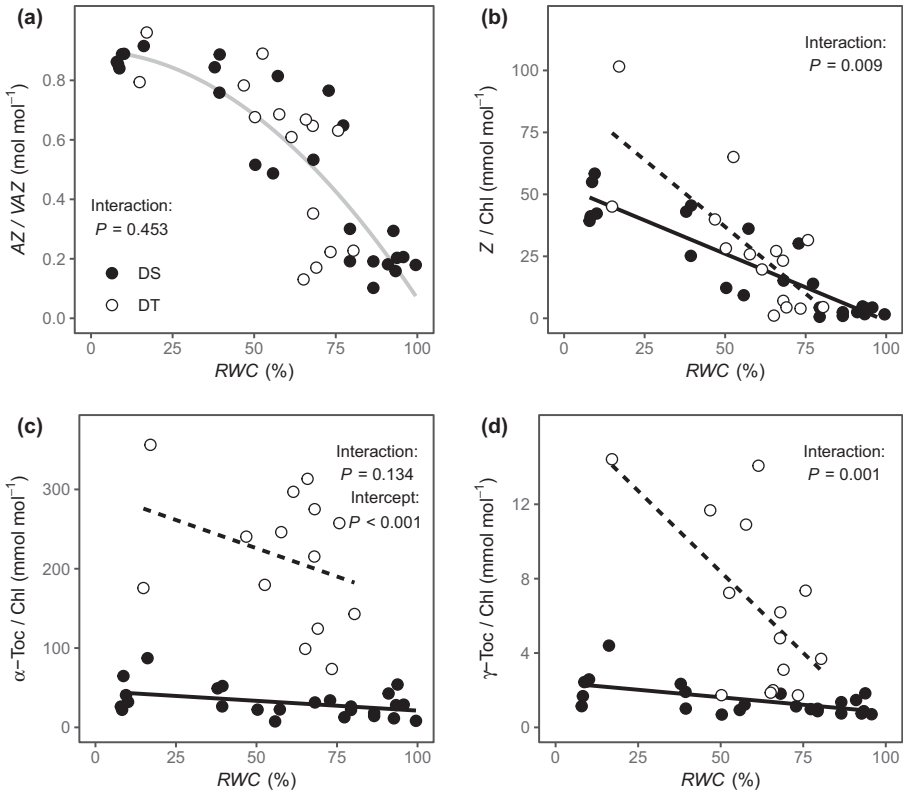

Fig. 5 Relationships between frond pigments and tocopherols and relative water content (*RWC*) of desiccation sensitive (DS) and desiccation tolerant (DT) fronds of *Anemia caffrorum* under water deficit stress. Filled circles correspond to DS fronds and open circles to DT fronds. The significance of the interaction (slope) and frond type (intercept) effects was determined using parametric ANCOVA and non-parametric ANCOVA for linear and quadratic fittings, respectively. *AZ* : *VAZ* ratio of the xanthophyll cycle (a): no differences among frond types; quadratic fitting for pooled data ($r^2 = 0.71$, $P < 0.001$). Zeaxanthin (*Z*) normalized by Chl*a* and Chl*b* content (b): significant differences among frond types; linear fittings for DS (solid line; $r^2 = 0.80$, $P < 0.001$) and DT (dashed line; $r^2 = 0.57$, $P = 0.001$). α-tocopherol normalized by Chl*a* and Chl*b* content (c): significant differences among frond types; linear fittings for DS (solid line; $r^2 = 0.15$, $P = 0.030$) and DT (dashed line; $r^2 = 0.24$, $P = 0.039$). γ-tocopherol normalized by Chl*a* and Chl*b* content (d): significant differences among frond types; linear fittings for DS (solid line; $r^2 = 0.34$, $P = 0.002$) and DT (dashed line; $r^2 = 0.31$, $P = 0.024$).

osmotic adjustment (Rodriguez-Dominguez *et al.*, 2016) from sugar and proline accumulation as in other resurrection ferns (Voytena *et al.*, 2014), although no clear changes in π_o were observed under WS. Another possible explanation for the increased osmotic effect in DT fronds could be the greater volume changes during dehydration (due to lower ϵ and higher shrinkage) that enable variation in osmotic potential without active solute accumulation (Munns, 1988). Hydraulic decline in leaves results from a combination of xylem and/or outer xylem conductance loss (Scoffoni *et al.*, 2017; Xiong & Nadal, 2020). Notably, embolism visualization using micro-computed tomography in the resurrection fern *Pentagramma triangularis* showed extensive cavitation at Ψ_{leaf} between −1 and −3 MPa, before other vascular modifications (Holmlund *et al.*, 2019), which is in the range of K_{plant} decline in *A. caffrorum*.

The ABA response in *A. caffrorum* resembled the pattern described for some conifer species, where ABA concentrations increase at moderate stress and decrease under severe dehydration (Brodribb & McAdam, 2013; Brodribb *et al.*, 2014). This response may be due to a reduction of foliar ABA production under severe water stress, possibly due to sensitivity of the synthetic apparatus to water potentials far below the turgor loss point. In conifer species this peak and decline of ABA was associated with a hydropassive stomatal closure during acute dehydration (Brodribb & McAdam, 2013). Indeed, most ferns display an ABA-independent mechanism of stomatal control (Brodribb & McAdam, 2011; McAdam & Brodribb, 2013). The burst of ABA under moderate stress may trigger some of the expression pathways for the induction of desiccation tolerance mechanisms (Giraola *et al.*, 2017), and increases in ABA have been reported in several resurrection species (Gaff & Loveys, 1984; Bartels *et al.*, 1990; Schiller *et al.*, 1997; Liu *et al.*, 2008), including the resurrection ferns *Cheilanthes myriophylla* (McAdam & Brodribb, 2013) and *Polypodium virginianum* (Reynolds & Bewley, 1993). The common ABA response in both DT and DS fronds shows that ABA increase is not exclusive to desiccation tolerance mechanisms and may also be related to leaf senescence (Lee *et al.*, 2011).

Constitutive and inducible protective mechanisms

Certain pigments, such as carotenoids and anthocyanins, together with other antioxidants provide resurrection plants with protection against photodamage (Fernández-Marín *et al.*, 2016; Oliver *et al.*, 2020). In *A. caffrorum*, DT fronds have an abaxial

coverage of light-protective hairs (Fig. 1d), which are exposed through frond curling as dehydration progresses. Together with a lower antennae size, as reflected by the higher Chl*a* : Chl*b* and β-Car : neoxanthin ratios, these could represent a strong accumulation of constitutive photoprotection mechanisms in DT fronds. Carotenes and tocopherols were found in larger proportions, indicating a stronger battery of lipophilic antioxidants in DT compared to DS fronds. In addition, inducible mechanisms upon desiccation were more evident in DT fronds. The rise in *AZ* : *VAZ*, which is typically induced by desiccation (Kranner *et al.*, 2002; Heber *et al.*, 2007; Fernández-Marín *et al.*, 2009, 2010, 2011, 2013, 2018; Beckett *et al.*, 2012) was common to both DT and DS fronds, reflecting a well-known photoprotection mechanism in plants during water stress (Fernández-Marín *et al.*, 2011, 2017a; Esteban *et al.*, 2015). However, this was more prominent in DT fronds. A similar observation can be made in comparing the DT fern *Asplenium ceterach* (Fernández-Marín *et al.*, 2009) with the DS fern *Asplenium scolopendrium* (Fernández-Marín *et al.*, 2011). Zeaxanthin plays a role in the preservation of the integrity of thylakoid membranes and the photosynthetic apparatus in the dry state (Fernández-Marín *et al.*, 2013), including a relevant role in the dissipation of excess energy as heat (Fernández-Marín *et al.*, 2010). The rise in tocopherol is a less widespread response to desiccation, but it has already been reported a number of times for lichens, ferns and angiosperms (Kranner *et al.*, 2002, 2003; Fernández-Marín *et al.*, 2011, 2020; López-Pozo *et al.*, 2019) and could play a key role in the protective responses that enable desiccation tolerance, as it seems to play in seeds (Seal *et al.*, 2010; Fernández-Marín *et al.*, 2017b). Overall, DT fronds of *A. caffrorum* seem to be physically and biochemically more protected against photooxidative risk than DS fronds.

An ecophysiological interpretation

The distinctive features observed between DT and DS fronds may point towards a different life strategy, which is determined by the fact that DT fronds occur during the hot dry season and DS fronds during the cold rainy season (Farrant *et al.*, 2009). One may think that DT fronds would present a set of features that delayed dehydration and provided more time to prepare for the desiccation stage (Oliver *et al.*, 1998); instead, they present much higher g_{min} and g_{sw} per *RWC* than DS fronds, indicating a selection towards rapid dehydration when soil water becomes limited. This further implies some degree of constitutive protection in DT fronds. Furthermore, rapid drying could be required to ensure appropriate concentration of select metabolites to form pockets of deep eutectic solvents, which in turn have been proposed to enable metabolic activity at low water contents and, ultimately, cytoplasmic vitrification (du Toit *et al.*, 2021). Enzymatic activity associated with photoprotective metabolism has been demonstrated at extremely low water contents in the lichen *Flavoparmelia caperata* (Carniel *et al.*, 2021), and such molecular mobility at low water contents is proposed to be a consistent feature of desiccation tolerance (Farrant & Hilhorst, 2021). Desiccation tolerant fronds can resume activity and recover *RWC* in the first 4–8 h after rehydration (Farrant *et al.*, 2009), which is much faster than reported in any angiosperm to date. Furthermore, in *A. caffrorum* the pathway for rehydration is probably more related to water absorption through the lamina surface rather than the petiole, as shown by the rehydration assays (Fig. S3). Some resurrection plants require apportion of water through the lamina surfaces for rapid and complete rehydration (Gaff, 1977; John & Hasenstein, 2017), although resurrection ferns still require water availability in the soil for a complete recovery (Holmlund *et al.*, 2020). Foliar water uptake may be enhanced by the presence of special structures, such as the peltate scales described in the resurrection fern *Pleopeltis polypodioides* that provide a wettable conduit for effective water uptake (John & Hasenstein, 2017). Desiccation tolerant fronds in *A. caffrorum* have similar structures on the abaxial surfaces, which are not found in DS fronds (Fig. 1e,f; detail in Farrant *et al.*, 2009). Presenting a high capacity for water absorption through the surface may imply a higher rate of water loss during dehydration, especially if the structures that enable rapid rehydration lose water at a similar rate (which is possible given the high g_{min} in DT fronds). These characteristics seem inappropriate during the dry season; however, fog events are well documented where *A. caffrorum* occurs (Roux, 1995), including Table Mountain, where *A. caffrorum* was collected (Marloth, 1905; Nagel, 1956). Moreover, the frequency of fog events is greater during the dry season in the distribution zone of *A. caffrorum* and can constitute a greater source of water than rainfall (Olivier, 2002).

The presence of DT fronds during the dry season, which can sustain rapid rehydration and recovery and resume positive carbon balance within 24 h, may enable *A. caffrorum* to effectively exploit the 'windows of opportunity' that certainly cannot be used by most annual plants that share the same habitat. On the other hand, the occurrence of DS fronds during the cool, wet winter, which present enhanced photosynthetic capacity and lower structural (i.e. *LMA*), antioxidant and photoprotection investment (and hence lower frond construction costs and higher carbon return), constitutes an efficient mechanism for investment into reproductive structures (and/or the rhizome) which are produced during the end of the rainy season and for the DT fronds produced at the start of the dry season (Farrant *et al.*, 2009). Such distinct foliar features could represent an extreme case of heteroblasty, which in some species is related to different carbon and water economics among leaves of the same plant (Zotz *et al.*, 2011). In this case, the foliar seasonality of *A. caffrorum* may confer competitive advantages in both summer and winter with coexisting annuals. However, the acquisition of desiccation tolerance possibly requires a higher resource investment in protective mechanisms such as thick cell walls (Nadal *et al.*, 2021), the maintenance of antioxidant capacity, and the production of polyphenols and LEA proteins, *inter alia*. Such a tolerance 'cost' would be counterproductive during the wet season. Given this unique adaptation, *A. caffrorum* constitutes an excellent organism in which to explore the physiological requirements and possible consequences associated with the adoption of desiccation tolerance.

Acknowledgements

This work was supported by the projects CTM2014-53902-C2-1-P from the Ministerio de Economía y Competitividad (MINECO, Spain) and the European Regional Development Fund (ERDF) and PGC2018-093824-B-C41/PGC2018-093824-B-C44 from the Ministerio de Ciencia, Innovación y Universidades (MCIU, Spain) and the ERDF; and the Basque Government (grant UPV/EHU IT-1018-16, Spain). MN was supported by the MINECO and the European Social Fund (pre-doctoral fellowship BES-2015-072578). AVP-C was supported by the Ministerio de Educación, Cultura y Deporte (MECD; pre-doctoral fellowship FPU-02054). MIA was supported by a pre-doctoral grant from the Basque Government. We thank the technical support for microscopy preparation provided by the Universitat de València (Secció de Microscopia Electrònica, SCSIE), Dr. Ferran Hierro (UIB, Serveis Cientificotècnics) and Margalida Roig Oliver (UIB). JMF provided funding for work conducted in South Africa from her South African Department of Science and Innovation, National Research Foundation Research Chair, grant no. 98406.

Author contributions

MN, JG, JMF and JF planned the research; MN, TJB, BF-M, JIG-P, MIA, ML-P and AVP-C performed the measurements; MN analysed the data and drafted the manuscript. All authors contributed to subsequent revisions and discussion.

ORCID

Tim J. Brodribb https://orcid.org/0000-0002-4964-6107
Jill M. Farrant https://orcid.org/0000-0002-1450-7967
Beatriz Fernández-Marín https://orcid.org/0000-0001-9951-0489
Jaume Flexas https://orcid.org/0000-0002-3069-175X
José I. García-Plazaola https://orcid.org/0000-0001-6498-975X
Miquel Nadal https://orcid.org/0000-0003-1472-1792
Alicia V. Perera-Castro https://orcid.org/0000-0001-8451-6052

Data availability

The data that support the findings of this study are available in the main manuscript and in the Supporting Information for this article.

References

Alpert P. 2006. Constraints of tolerance: why are desiccation-tolerant organisms so small or rare? *The Journal of Experimental Biology* **209**: 1575–1584.

Alpert P, Oliver MJ. 2002. Drying without dying. In: Black M, Pritchard HW, eds. *Desiccation and survival in plants – drying without dying*. Wallingford, UK; New York, NY, USA: CABI Publishing, 3–43.

Bartels D, Schneider K, Terstappen G, Piatkowski D, Salamini F. 1990. Molecular cloning of abscisic acid-modulated genes which are induced during desiccation of the resurrection plant *Craterostigma plantagineum*. *Planta* **181**: 27–34.

Beckett M, Loreto F, Velikova V, Brunetti C, Di Ferdinando M, Tattini M, Calfapietra C, Farrant JM. 2012. Photosynthetic limitations and volatile and non-volatile isoprenoids in the poikilochlorophyllous resurrection plant *Xerophyta humilis* during dehydration and rehydration. *Plant, Cell & Environment* **35**: 2061–2074.

Brodribb TJ, McAdam SAM. 2011. Passive origins of stomatal control in vascular plants. *Science* **331**: 582–585.

Brodribb TJ, McAdam SAM. 2013. Abscisic acid mediates a divergence in the drought response of two conifers. *Plant Physiology* **162**: 1370–1377.

Brodribb TJ, McAdam SAM, Jordan GJ, Martins SCV. 2014. Conifer species adapt to low-rainfall climates by following one of two divergent pathways. *Proceedings of the National Academy of Sciences, USA* **111**: 14489–14493.

Buckley TN, Diaz-Espejo A. 2015. Partitioning changes in photosynthetic rate into contributions from different variables. *Plant, Cell & Environment* **38**: 1200–1211.

Buckley TN, Mott KA, Farquhar GD. 2003. A hydromechanical and biochemical model of stomatal conductance. *Plant, Cell & Environment* **26**: 1767–1785.

Carniel FC, Fernandez-Marín B, Arc E, Craighero T, Laza JM, Incerti G, Tretiach M, Kranner I. 2021. How dry is dry? Molecular mobility in relation to thallus water content in a lichen. *Journal of Experimental Botany* **72**: 1576–1588.

Dinakar C, Djilianov D, Bartels D. 2012. Photosynthesis in desiccation tolerant plants: energy metabolism and antioxidative stress defense. *Plant Science* **182**: 29–41.

Esteban R, Barrutia O, Artextxe U, Fernández-Marín B, Hernández A, García-Plazaola JI. 2015. Internal and external factors affecting photosynthetic pigment composition in plants: a meta-analytical approach. *New Phytologist* **206**: 268–280.

Evans JR, von Caemmerer S, Setchell BA, Hudson GS. 1994. The relationship between CO_2 transfer conductance and leaf anatomy in transgenic tobacco with a reduced content of Rubisco. *Australian Journal of Plant Physiology* **21**: 475–495.

Evans JR, Clarke VC. 2019. The nitrogen cost of photosynthesis. *Journal of Experimental Botany* **70**: 7–15.

Farrant JM. 2000. A comparison of mechanisms of desiccation tolerance among three angiosperm resurrection plant species. *Plant Ecology* **151**: 29–39.

Farrant JM, Brandt W, Lindsey GG. 2007. An overview of mechanisms of desiccation tolerance in selected angiosperm resurrection plants. *Plant Stress* **1**: 72–84.

Farrant JM, Hilhorst HWM. 2021. What is dry? Exploring molecular mobility at very low water contents. *Journal of Experimental Botany* **72**: 1507–1510.

Farrant JM, Lehner A, Cooper K, Wiswedel S. 2009. Desiccation tolerance in the vegetative tissues of the fern *Mohria caffrorum* is seasonally regulated. *The Plant Journal* **57**: 65–79.

Fernández-Marín B, Balaguer L, Esteban R, Becerril JM, García-Plazaola JI. 2009. Dark induction of the photoprotective xanthophyll cycle in response to dehydration. *Journal of Plant Physiology* **166**: 1734–1744.

Fernández-Marín B, Becerril JM, García-Plazaola JI. 2010. Unravelling the roles of desiccation-induced xanthophyll cycle activity in darkness: a case study in *Lobaria pulmonaria*. *Planta* **231**: 1335–1342.

Fernández-Marín B, Hernández A, García-Plazaola JI, Esteban R, Míguez F, Artetxe U, Gómez-Sagasti MT. 2017a. Photoprotective strategies of Mediterranean plants in relation to morphological traits and natural environmental pressure: a meta-analytical approach. *Frontiers in Plant Science* **8**: 1051.

Fernández-Marín B, Holzinger A, García-Plazaola JI. 2016. Photosynthesis strategies of desiccation-tolerant organisms. In: Pessarakli M, ed. *Handbook of photosynthesis*. Boca Raton, FL, USA: CRC Press, 663–681.

Fernández-Marín B, Kranner I, Sebastián MS, Artetxe U, Laza JM, Vilas JL, Pritchard HW, Nadajaran J, Míguez F, Becerril JM *et al.* 2013. Evidence for the absence of enzymatic reactions in the glassy state. A case study of xanthophyll cycle pigments in the desiccation-tolerant moss *Syntrichia ruralis*. *Journal of Experimental Botany* **64**: 3033–3043.

Fernández-Marín B, Míguez F, Becerril JM, García-Plazaola JI. 2011. Dehydration-mediated activation of the xanthophyll cycle in darkness: is it related to desiccation tolerance? *Planta* **234**: 579–588.

Fernández-Marín B, Míguez F, Méndez-Fernández L, Agut A, Becerril JM, García-Plazaola JI, Kranner I, Colville L. 2017b. Seed carotenoid and tocochromanol composition of wild Fabaceae species is shaped by phylogeny and ecological factors. *Frontiers in Plant Science* **8**: 1–16.

Fernández-Marín B, Nadal M, Gago J, Fernie AR, López-Pozo M, Artetxe U, García-Plazaola JI, Verhoeven A. 2020. Born to revive: molecular and physiological mechanisms of double tolerance in a paleotropical and resurrection plant. *New Phytologist* **226**: 741–759.

Fernández-Marín B, Neuner G, Kuprian E, Laza JM, García-Plazaola JI, Verhoeven A. 2018. First evidence of freezing tolerance in a resurrection plant: insights into molecular mobility and zeaxanthin synthesis in the dark. *Physiologia Plantarum* **163**: 472–489.

Flexas J, Carriquí M, Nadal M. 2018. Gas exchange and hydraulics during drought in crops: who drives whom? *Journal of Experimental Botany* **69**: 3791–3795.

Flexas J, Díaz-Espejo A, Berry JA, Cifre J, Galmés J, Kaldenhoff R, Medrano H, Ribas-Carbó M. 2007. Analysis of leakage in IRGA's leaf chambers of open gas exchange systems: quantification and its effects in photosynthesis parameterization. *Journal of Experimental Botany* **58**: 1533–1543.

Gaff DF. 1977. Desiccation tolerant vascular plants of Southern Africa. *Oecologia* **31**: 95–109.

Gaff DF, Loveys BR. 1984. Abscisic acid content and effects during dehydration of detached leaves of desiccation tolerant plants. *Journal of Experimental Botany* **35**: 1350–1358.

Gaff DF, Oliver M. 2013. The evolution of desiccation tolerance in angiosperm plants: a rare yet common phenomenon. *Functional Plant Biology* **40**: 315–328.

Gago J, Carriquí M, Nadal M, Clemente-Moreno MJ, Coopman RE, Fernie AR, Flexas J. 2019. Photosynthesis optimized across land plant phylogeny. *Trends in Plant Science* **24**: 947–958.

Gago J, Coopman RE, Cabrera HM, Hermida C, Molins A, Conesa MÀ, Galmés J, Carbó-Ribas M, Flexas J. 2013. Photosynthesis limitations in three fern species. *Physiologia Plantarum* **149**: 599–611.

García-Plazaola JI, Becerril JM. 2001. Seasonal changes in photosynthetic pigments and antioxidants in beech (*Fagus sylvatica*) in a Mediterranean climate: implications for tree decline diagnosis. *Australian Journal of Plant Physiology* **28**: 225–232.

Giraola V, Hou Q, Bartels D. 2017. Angiosperm plant desiccation tolerance. Hints from transcriptomics and genome sequencing. *Trends in Plant Science* **22**: 705–717.

Grassi G, Magnani F. 2005. Stomatal, mesophyll conductance and biochemical limitations to photosynthesis as affected by drought and leaf ontogeny in ash and oak trees. *Plant, Cell & Environment* **28**: 834–849.

Heber U, Azarkovich M, Shuvalov V. 2007. Activation of mechanisms of photoprotection by desiccation and by light: poikilohydric photoautotrophs. *Journal of Experimental Botany* **58**: 2745–2759.

Hoekstra FA, Golovina EA, Buitink J. 2001. Mechanisms of plant desiccation tolerance. *Trends in Plant Science* **6**: 431–438.

Holmlund HI, Davis SD, Ewers FW, Aguirre NM, Sapes G, Sala A, Pittermann J. 2020. Positive root pressure is critical for whole-plant desiccation recovery in two species of terrestrial resurrection ferns. *Journal of Experimental Botany* **71**: 1139–1150.

Holmlund HI, Pratt RB, Jacobsen AL, Davis SD, Pittermann J. 2019. High-resolution computed tomography reveals dynamics of desiccation and rehydration in fern petioles of a desiccation-tolerant fern. *New Phytologist* **224**: 97–105.

John SP, Hasenstein KH. 2017. The role of peltate scales in desiccation tolerance of *Pleopeltis polypodioides*. *Planta* **245**: 207–220.

Kranner I, Beckett RP, Wornik S, Zorn M, Pfeifhofer HW. 2002. Revival of a resurrection plant correlates with its antioxidant status. *The Plant Journal* **31**: 13–24.

Kranner I, Zorn M, Turk B, Wornik S, Beckett RP, Batič F. 2003. Biochemical traits of lichens differing in relative desiccation tolerance. *New Phytologist* **160**: 167–176.

Lee IC, Hong SW, Whang SS, Lim PO, Nam HG, Koo JC. 2011. Age-dependent action of an ABA-inducible receptor kinase, RPK1, as a positive regulator of senescence in *Arabidopsis* leaves. *Plant and Cell Physiology* **52**: 651–662.

Liu MS, Chien CT, Lin TP. 2008. Constitutive components and induced gene expression are involved in the desiccation tolerance of *Selaginella tamariscina*. *Plant and Cell Physiology* **49**: 653–663.

López-Pozo M, Fernández-Marín B, García-Plazola JI, Ballesteros D. 2018. Desiccation tolerance in ferns: from the unicellular spore to the multi-tissular sporophyte. In: Fernández H, ed. *Current advances in fern research*. Cham, Switzerland: Springer, 401–426.

López-Pozo M, Gasulla F, García-Plazaola JI, Fernández-Marín B. 2019. Unraveling metabolic mechanisms behind chloroplast desiccation tolerance: chlorophyllous fern spore as a new promising unicellular model. *Plant Science* **281**: 251–260.

Marloth R. 1905. Results of further experiments on Table Mountain for ascertaining the amount of moisture deposited from the southeast clouds. *Transactions of the South African Philosophical Society* **16**: 97–105.

McAdam SAM, Brodribb TJ. 2012. Fern and lycophyte guard cells do not respond to endogenous abscisic acid. *The Plant Cell* **24**: 1510–1521.

McAdam SAM, Brodribb TJ. 2013. Ancestral stomatal control results in a canalization of fern and lycophyte adaptation to drought. *New Phytologist* **198**: 429–441.

Melkonian JJ, Wolfe J, Steponkus PL. 1982. Determination of the volumetric modulus of elasticity of wheat leaves by pressure-volume relations and the effect of drought conditioning. *Crop Science* **22**: 116–123.

Moore JP, Nguema-Ona EE, Vicré-Gibouin M, Sørensen I, Willats WGT, Driouich A, Farrant JM. 2013. Arabinose-rich polymers as an evolutionary strategy to plasticize resurrection plant cell walls against desiccation. *Planta* **237**: 739–754.

Moore JP, Vicré-Gibouin M, Farrant JM, Driouich A. 2008. Adaptations of higher plant cell walls to water loss: drought vs desiccation. *Physiologia Plantarum* **134**: 237–245.

Mundree SG, Farrant JM. 2000. Some physiological and molecular insights into the mechanisms of desiccation tolerance in the resurrection plant *Xerophyta viscosa* Baker. In: Cherry JH, Locy RD, Rychter A eds. *Plant tolerance to abiotic stress in agriculture: role of genetic engineering*. NATO Science Series, vol. 83. Dordrecht, the Netherlands: Springer, 201–222.

Munns R. 1988. Why measure osmotic adjustment? *Australian Journal of Plant Physiology* **15**: 717–726.

Muslin EH, Homann PH. 1992. Light as a hazard for the desiccation-resistant 'resurrection' fern *Polypodium polypodioides* L. *Plant, Cell & Environment* **15**: 81–89.

Nadal M, Flexas J. 2019. Variation in photosynthetic characteristics with growth form in a water-limited scenario: implications for assimilation rates and water use efficiency in crops. *Agricultural Water Management* **216**: 457–472.

Nadal M, Flexas J, Gulías J. 2018. Possible link between photosynthesis and leaf modulus of elasticity among vascular plants: a new player in leaf traits relationships? *Ecology Letters* **21**: 1372–1379.

Nadal M, Perera-Castro AV, Gulías J, Farrant JM, Flexas J. 2021. Resurrection plants optimize photosynthesis despite very thick cell walls by means of chloroplast distribution. *Journal of Experimental Botany* **72**: 2600–2610.

Nagel JF. 1956. Fog precipitation on Table Mountain. *Quarterly Journal of the Royal Meteorological Society* **82**: 452–460.

Niinemets Ü. 2001. Global-scale climatic controls of leaf dry mass per area, density, and thickness in trees and shrubs. *Ecology* **82**: 453–469.

Oliver MJ, Farrant JM, Hilhorst HWM, Mundree S, Williams B, Bewley JD. 2020. Desiccation tolerance: avoiding cellular damage during drying and rehydration. *Annual Review of Plant Biology* **71**: 435–460.

Oliver MJ, O'Mahony P, Wood AJ 1998. "To dryness and beyond"–preparation for the dried state and rehydration in vegetative desiccation-tolerant plants. *Plant Growth Regulation* **24**: 193–201.

Oliver MJ, Tuba Z, Mishler BD. 2000. The evolution of vegetative desiccation tolerance in land plants. *Plant Ecology* **151**: 85–100.

Olivier J. 2002. Fog-water harvesting along the West Coast of South Africa: a feasibility study. *Water SA* **28**: 349–360.

Onoda Y, Schieving F, Anten NPR. 2015. A novel method of measuring leaf epidermis and mesophyll stiffness shows the ubiquitous nature of the sandwich structure of leaf laminas in broad-leaved angiosperm species. *Journal of Experimental Botany* **66**: 2487–2499.

Onoda Y, Wright IJ, Evans JR, Hikosaka K, Kitajima K, Niinemets Ü, Poorter H, Tosens T, Westoby M. 2017. Physiological and structural tradeoffs underlying the leaf economics spectrum. *New Phytologist* **214**: 1447–1463.

Peeva V, Cornic G. 2009. Leaf photosynthesis of *Haberlea rhodopensis* before and during drought. *Environmental and Experimental Botany* **65**: 310–318.

Pérez-Harguindeguy N, Díaz S, Garnier E, Lavorel S, Poorter H, Jaureguiberry P, Bret-Harte MS, Cornwell WK, Craine JM, Gurvich DE *et al.* 2013. New handbook for standardised measurement of plant functional traits worldwide. *American Journal of Botany* **61**: 167–234.

Porembski S. 2011. Evolution, diversity, and habitats of Poikilohydrous vascular plants. In: Lüttge U, Beck E, Bartels D, eds. *Plant desiccation tolerance, ecological studies, vol. 215*. Heidelberg, Germany: Springer, 139–154.

Proctor MCF, Tuba Z. 2002. Poikilohydry and homoihydry: antithesis or spectrum of possibilities? *New Phytologist* **156**: 327–349.

R Core Team. 2019. *R: a language and environment for statistical computing*. Vienna, Austria: R Foundation for Statistical Computing.

Ramírez-Valiente JA, López R, Hipp AL, Aranda I. 2020. Correlated evolution of morphology, gas exchange, growth rates and hydraulics as a response to precipitation and temperature regimes in oaks (*Quercus*). *New Phytologist* **227**: 794–809.

Rapparini F, Neri L, Mihailova G, Petkova S, Georgieva K. 2015. Growth irradiance affects the photoprotective mechanisms of the resurrection angiosperm *Haberlea rhodopensis* Friv. in response to desiccation and rehydration at morphological, physiological and biochemical levels. *Environmental and Experimental Botany* **113**: 67–79.

Reynolds TL, Bewley JD. 1993. Abscisic acid enhances the ability of the desiccation-tolerant fern *Polypodium virginianum* to withstand drying. *Journal of Experimental Botany* **44**: 1771–1779.

Rodriguez-Dominguez CM, Buckley TN, Egea G, de Cires A, Hernandez-Santana V, Martorell S, Diaz-Espejo A. 2016. Most stomatal closure in woody species under moderate drought can be explained by stomatal responses to leaf turgor. *Plant, Cell & Environment* **39**: 2014–2026.

Roux JP. 1995. Systematic studies in the genus *Mohria* (Pteridophyta: Anemiaceae). VI. Taxonomic review. *Bothalia* **25**: 1–12.

Sack L, Pasquet-Kok J. 2011. *PrometheusWiki. Leaf pressure-volume curve parameters*. [WWW document] URL http://prometheuswiki.org/tiki-page history.php?page=Leaf%20pressure-volume%20curve%20parameters&previe w=16. [accessed 10 April 2018].

Sack L, Scoffoni C. 2011. *PrometheusWiki. Minimum epidermal conductance (gmin, a.k.a. cuticular conductance)*. [WWW document] URL http://promethe uswiki.org/tiki-pagehistory.php?page=Minimum%20epidermal%20conducta nce%20(gmin,%20a.k.a.%20cuticular%20conductance)&preview=7. [accessed 10 April 2018].

Saito T, Soga K, Hoson T, Terashima I. 2006. The bulk elastic modulus and the reversible properties of cell walls in developing *Quercus* leaves. *Plant and Cell Physiology* **47**: 715–725.

Schiller P, Heilmeier H, Hartung W. 1997. Abscisic acid (ABA) relations in the aquatic resurrection plant *Chamaegigas intrepidus* under naturally fluctuating environmental conditions. *New Phytologist* **136**: 603–611.

Schwab KB, Schreiber U, Heber U. 1989. Response of photosynthesis and respiration of resurrection plants to desiccation and rehydration. *Planta* **177**: 217–227.

Scoffoni C, Albuquerque C, Brodersen CR, Townes SV, John GP, Bartlett MK, Buckley TN, McElrone AJ, Sack L. 2017. Outside-xylem vulnerability, not xylem embolism, controls leaf hydraulic decline during dehydration. *Plant Physiology* **173**: 1197–1210.

Scoffoni C, Vuong C, Diep S, Cochard H, Sack L. 2014. Leaf shrinkage with dehydration: coordination with hydraulic vulnerability and drought tolerance. *Plant Physiology* **164**: 1772–1788.

Seal CE, Zammit R, Scott P, Flowers TJ, Kranner I. 2010. Glutathione half-cell reduction potential and α-tocopherol as viability markers during the prolonged storage of *Suaeda maritima* seeds. *Seed Science Research* **20**: 47–53.

Sharkey TD. 2016. What gas exchange data can tell us about photosynthesis. *Plant, Cell & Environment* **39**: 1161–1163.

Sherwin HW, Farrant JM. 1998. Protection mechanisms against excess light in the resurrection plants *Craterostigma wilmsii* and *Xerophyta viscosa*. *Plant Growth Regulation* **24**: 203–210.

Shivaraj YN, Barbara P, Gugi B, Vicré-Gibouin M, Driouich A, Govind SR, Devaraja A, Kambalagere Y. 2018. Perspectives on structural, physiological, cellular, and molecular responses to desiccation in resurrection plants. *Scientifica* **2018**: 9464592.

Shoko R. 2015. *A proteomic investigation of the rhizomes of the resurrection fern* Mohria caffrorum *L. (Desv.) in response to desiccation*. PhD thesis, University of Cape Town, South Africa.

Terashima I, Hanba YT, Tholen D, Niinemets Ü. 2011. Leaf functional anatomy in relation to photosynthesis. *Plant Physiology* **155**: 108–116.

Thain JF. 1983. Curvature correction factors in the measurement of cell surface areas in plant tissues. *Journal of Experimental Botany* **34**: 87–94.

Théroux-Rancourt G, Éthier G, Pepin S. 2015. Greater efficiency of water use in poplar clones having a delayed response of mesophyll conductance to drought. *Tree Physiology* **35**: 172–184.

du Toit SF, Bentley J, Farrant JM. 2021. NADES formation in vegetative desiccation tolerance: prospects and challenges. In: Verpoorte R, Witkamp G, Choi YH, eds. *Advances in botanical research. Eutectic solvents and stress in plants*. London, UK: Academic Press, 225–252.

Tomàs M, Flexas J, Copolovici L, Galmés J, Hallik L, Medrano H, Ribas-Carbó M, Tosens T, Vislap V, Niinemets Ü. 2013. Importance of leaf anatomy in determining mesophyll diffusion conductance to CO_2 across species: quantitative limitations and scaling up by models. *Journal of Experimental Botany* **64**: 2269–2281.

Trueba S, Pan R, Scoffoni C, John GP, Davis SD, Sack L. 2019. Thresholds for leaf damage due to dehydration: declines of hydraulic function, stomatal conductance and cellular integrity precede those for photochemistry. *New Phytologist* **223**: 134–149.

Tuba Z, Lichtenthaler HK, Zs C, Nagy Z, Szente K. 1996. Loss of chlorophylls, cessation of photosynthetic CO_2 assimilation and respiration in the poikilochlorophyllous plant *Xerophyta scabrida* during desiccation. *Physiologia Plantarum* **96**: 383–388.

Vicré M, Farrant JM, Driouich A. 2004. Insights into the cellular mechanisms of desiccation tolerance among angiosperm resurrection plant species. *Plant, Cell & Environments* **27**: 1329–1340.

Voytena APL, Minardi BD, Barufi JB, Santos M, Randi AM. 2014. *Pleopeltis pleopeltifolia* (Polypodiopsida, Polypodiaceae), a poikilochlorophyllous desiccation-tolerant fern: anatomical, biochemical and physiological responses during water stress. *Australian Journal of Botany* **62**: 647–656.

Wang X. 2020. *fANCOVA: nonparametric analysis of covariance*. R package v.0.6-1. [WWW document] URL https://CRAN.R-project.org/package=f ANCOVA [accessed 1 March 2021].

Wang X, Du T, Huang J, Peng S, Xiong D. 2018. Leaf hydraulic vulnerability triggers the decline in stomatal and mesophyll conductance during drought in rice. *Journal of Experimental Botany* **69**: 4033–4045.

Xiong D, Nadal M. 2020. Linking water relations and hydraulics with photosynthesis. *The Plant Journal* **101**: 800–815.

Zia A, Walker BJ, Oung HMO, Charuvi D, Jahns P, Cousins AB, Farrant JM, Reich Z, Kirchhoff H. 2016. Protection of the photosynthetic apparatus against dehydration stress in the resurrection plant *Craterostigma pumilum*. *The Plant Journal* **87**: 664–680.

Zotz G, Wilhelm K, Becker A. 2011. Heteroblasty – a review. *The Botanical Review* **77**: 109–151.

Supporting Information

Additional Supporting Information may be found online in the Supporting Information section at the end of the article.

Fig. S1 Photosynthetic response to rapid dehydration in detached fronds.

Fig. S2 Monitoring of soil moisture measured using a humidity probe during the water stress cycle.

Fig. S3 Rehydration test in desiccation tolerant (DT) fronds.

Table S1 Rapid response to dehydration in excised fronds from well-watered plants.

Please note: Wiley Blackwell are not responsible for the content or functionality of any Supporting Information supplied by the authors. Any queries (other than missing material) should be directed to the *New Phytologist* Central Office.